

NTATION PAGE

Form Approved
OMB No. 0704-0188

2

AD-A232 964

ited to average 1 hour per response, including the time for reviewing instructions, searching existing data sources, reviewing the collection of information. Send comments regarding this burden estimate or any other aspect of this burden, to Washington Headquarters Services, Directorate for Information Operations and Reports, 1215 Jefferson Office of Management and Budget, Paperwork Reduction Project (0704-0188), Washington, DC 20503.

RT DATE

28 JAN 91

3. REPORT TYPE AND DATES COVERED

Final, 1 JUL 90 - 31 DEC 90

4. TITLE AND SUBTITLE

DEVELOPMENT OF MINIATURE TEMPERATURE SENSORS

5. FUNDING NUMBERS

Contract No.
DAAL 03-90-C-0012

6. AUTHOR(S)

MARY G. MOSS*, RYAN E. GIEDD**, AND TERRY BREWER*

7. PERFORMING ORGANIZATION NAME(S) AND ADDRESS(ES)

* BREWER SCIENCE, INC PO Box GG, 2401 High Tech Drive
Rolla, Missouri 65401 and
**SOUTHWEST MISSOURI STATE UNIVERSITY
901 S. NATIONAL
Springfield, Missouri 65804

8. PERFORMING ORGANIZATION REPORT NUMBER

NONE

9. SPONSORING/MONITORING AGENCY NAME(S) AND ADDRESS(ES)

SPONSORED BY SDIO,
ADMINISTERED BY U.S. ARMY RESEARCH OFFICE
PO Box 12211
Research Triangle Park, NC 27709-2211

10. SPONSORING/MONITORING AGENCY REPORT NUMBER

ARO 28081.1-EC-S&I

11. SUPPLEMENTARY NOTES

12a. DISTRIBUTION/AVAILABILITY STATEMENT

APPROVED FOR PUBLIC RELEASE / DISTRIBUTION UNLIMITED

12b. DISTRIBUTION CODE

\$

MAR 1 8 1991

G

13. ABSTRACT (Maximum 200 words)

Phase I work demonstrated temperature sensors formed from polyacrylonitrile and similar polymers which could be applied from solution onto a substrate, then subsequently ion implanted to have conductivity in the kilohm to megaohm/square range. If desired, the films could be patterned before implantation to small geometries by lithographic procedures. The resulting films had a large, negative temperature coefficient of resistance, and the resistance-temperature response was reproducible and retraceable within experimental error over multiple cycles. The films were extremely durable and solvent-resistant. A quasi-one dimensional hopping mechanism for conduction was indicated from the conductivity versus temperature and conductivity versus pressure measurements. Hall effect measurements showed n-type conductivity. The films were homogeneous on a one micron scale, as shown by an SEM photomicrograph, indicating that the ion implanted films could be used as small geometry temperature sensors.

14. SUBJECT TERMS

TEMPERATURE SENSORS, ION IMPLANTATION, CONDUCTING POLYMERS

15. NUMBER OF PAGES

26

16. PRICE CODE

17. SECURITY CLASSIFICATION OF REPORT

UNCLASSIFIED

18. SECURITY CLASSIFICATION OF THIS PAGE

UNCLASSIFIED

19. SECURITY CLASSIFICATION OF ABSTRACT

UNCLASSIFIED

20. LIMITATION OF ABSTRACT

UI

DTIC FILE COPY

FINAL REPORT

"Development of Miniature Temperature Sensors"

Mary G. Moss,¹ Ryan E. Giedd,² Kim Moeckli,¹
and Terry Brewer¹

¹Brewer Science, Inc.,
P. O. Box GG, 2401 High Tech Drive
Rolla, Missouri 65401

²Department of Physics and Astronomy
Southwest Missouri State University
901 S. National
Springfield, MO 65804

January 30, 1991

Contract No.: DAAL03-90-C-0012
Effective Date of contract: July 1, 1990
Expiration Date of contract: December 31, 1990
Principal Investigator: Mary G. Moss (314) 364-0300

Accession For	
NTIS CRA&I	<input checked="checked" type="checkbox"/>
DTIC TAB	<input type="checkbox"/>
Unannounced	<input type="checkbox"/>
Justification	
By	
Distribution/	
Availability Codes	
Dist	Avail and/or Special
A-1	

I. Introduction

Temperature sensors are required for a variety of applications in which information is provided to a control circuit which compensates for temperature changes. In many applications, small, compact sensors with a low thermal time constant are required. To ensure good heat transfer, the sensors must be in close thermal contact with the object whose temperature is to be measured. One solution to these requirements is a film with a resistance which is highly dependent upon temperature, and which is directly deposited onto the substrate.

During Phase I, we demonstrated such temperature sensing elements made from organic polymers which were deposited from solution, then made conductive by ion implantation. Organic polymers are typically insulators, but they can be made conductive by inducing carbonized areas by pyrolysis or by ion implantation. In particular, ion implanted polymers are known to have a resistance which is exponentially dependent upon the temperature.¹ Giedd et al. recently demonstrated a stable, high temperature coefficient of resistance in an ion implanted polymer, polyethylene terephthalate (PET).² PET, however, was not organic solvent-soluble and could not be deposited from solution. In order to make temperature sensors which could be more easily deposited onto a substrate, solvent-soluble polymers were chosen for testing in Phase I.

The technical objectives of Phase I were as follows:

- To show that spin-coated films of polyacrylonitrile or similar polymers could be made conductive by ion implantation,
- To show that the conductivity varied over a large temperature range, in a manner similar to commercial thermistors,
- To determine whether the variation could be used to measure temperature reproducibly.

These objectives were achieved, and the results are described in the following report. Portions of these results were presented at the IBBM meeting at Knoxville, Tennessee, in September 1990.³

II. Experimental Methods

Polymers were selected on the basis of their ability to be conveniently processed from solution and on the basis of their potential to form conductive films by pyrolysis or ion implantation. Table 1 lists the polymers which were selected and their abbreviations. They included two polymers which contained acrylonitrile (poly(acrylonitrile-co-methyl

methacrylate) and poly(styrene-acrylonitrile)), polysulfone, and a precursor resin which could be pyrolyzed on heating to form a conjugated, conducting polymer, designated as NRL resin.

Polymers were dissolved in a suitable solvent, filtered, and spin-coated onto glass microscope slides. The slides were baked on a hotplate to remove residual solvent, and thicknesses were measured using a Dektak surface profilometer. Film thicknesses ranged from 0.2 to 1.0 micron.

Films were ion implanted with 50 keV Ar^+ , B^+ , or As^+ ions. Fluences ranged from 2×10^{16} to 1×10^{17} ions/cm². The range of ions in the film was determined from TRIM calculations.⁴ The thickness of the electrically active layer was taken to be the mean range of the ions in the material. Since all of the polymers had approximately equal densities, this range was primarily dependent upon the ion mass and energy. For argon ions, this range was calculated to be 0.067 micrometer; for boron ions, 0.225 micrometer; and for arsenic ions, 0.075 micrometer. Film thicknesses were greater than any of these ranges, except for the boron-implanted NRL resins. The thickness of the NRL films was limited by the low solubility of the resin in the spin-coating solution.

Electrical contacts to the polymer films were made by evaporating four metal electrodes across the polymer films. The electrodes were approximately 0.3 cm in width and separated by 0.7 cm. Resistances were measured with a Hewlett-Packard 4261A LCR meter. Three measurements of resistance were taken per sample; these results were plotted versus electrode separation to give a linear relationship. The slope of this plot was a quantity equal to the bulk resistivity/(thickness x width of sample). Multiplication by the sample width (25.4 mm) gave the surface resistance in ohms/square. This method was chosen rather than a four-probe technique to eliminate the pressure-dependent resistance and film damage that is sometimes a problem when measuring the resistance of polymer films with a sharp probe. Determination of contact resistance is described later.

For measurements of resistance at temperatures above room temperature, the sample was heated on a Temptronic thermochuck. The resistance was measured with an HP LCR meter, or for the higher impedance samples, with a Keithley model 614 ohmmeter. Measurements were conducted in ambient air.

Over the shorter temperature ranges, the slope of the the plot of the natural log of the surface resistance versus $1/\text{temperature}$ was calculated. The slope is designated as β

in thermistor literature, and is related to the temperature coefficient of resistance, defined as:

$$\alpha = (1/R_T) dR_T/dT = -\beta/T^2$$

The data actually had better fit to a square root of $1/\text{temperature}$ dependence, as described later, but over the 25-100°C range the above dependence was linear. Beta values which were calculated from these measurements had errors of approximately 3% due to thermal variations and ohmmeter accuracy.

Resistance-temperature measurements at cryogenic temperatures were performed using a closed-cycle helium refrigerator. The sample and the temperature sensor were kept in equilibrium by using 1 atm of helium exchange gas in the sample chamber. The temperature measurements were made by a calibrated platinum resistor accurate to $\pm 1\text{K}$ in this temperature range.

III. Results

Argon-implanted samples

The initial samples were implanted with argon, which was expected to be an inert species capable of producing a lot of localized film damage because of its large size. In order to determine approximate implantation conditions, the final film resistance of polyacrylonitrile was characterized as a function of the fluence (2×10^{16} to 1×10^{17} ions/cm²), the beam current (300 and 500 microamps), and the film thickness (0.3 and 1.0 micrometer).

Following implantation with argon, the resistance decreased many orders of magnitude to a final value of 79 megohms/square. The resistance decreased rapidly with fluence until a saturation resistance was reached. This behavior is typical of ion-implanted polymers.⁵ The maximum attainable resistance of PAN was a function of the total fluence (defined as the integral of the beam current over time divided by the area), and was relatively independent of the beam current itself. The thickness of the sample had little effect on the resistance. The results are shown in Figure 1.

Other spin-coated films which were implanted with argon ions, including poly(styrene-acrylonitrile), polysulfone, and a poly(azomethine), had a similar resistance-fluence relationship. The resistance is shown as a function of fluence for poly(styrene-acrylonitrile) (Figure 2), polysulfone (Figure 3), and polyazomethine (Figure 4).

All of the films exhibited a large, negative temperature coefficient of resistance. The film resistance and beta values (slope of the $\ln(R)$ vs. $1/T$ plot over the 25°-100°C temperature range) are listed in Table 2 for the argon ion-implanted samples. The change of resistance with temperature was approximately -0.5%/°C for polyacrylonitrile and poly(styrene-acrylonitrile.)

After five temperature recycles of newly implanted samples, the slope of the plot exhibited a steadily decreasing value to a maximum change of 10%. Samples which had stabilized over a period of time had a resistance-temperature relationship which was much more stable to recycling. These samples had random changes from cycle to cycle within experimental error. Large increases in resistance of the argon-implanted films were evident after storage in the ambient atmosphere.

While the argon-implanted poly(acrylonitrile) and poly(styrene-acrylonitrile) films were conductive and had a high resistance-temperature dependence, film quality was not good. All of the films had visible pinholes which appeared the day following implantation. The reason for the pinhole formation was unclear. Annealing the films to remove volatile solvent prior to implantation did not improve the film quality. Implantation is known to generate quantities of volatile gas such as hydrogen, but it is unlikely that these gases would cause delayed film quality problems.

In order to improve the film quality, other implant ions were tested. Implantation with boron and arsenic ions caused no such pinhole formation, and resulted in tough, high quality films.

Boron and arsenic ion implantation

Changing the dopant ion to boron resulted in good quality films. The majority of the remaining work was conducted with boron-implanted samples, although arsenic was also found to be an effective implant ion.

Films of poly(styrene-acrylonitrile), PAN, and the NRL resin were implanted with boron ions under the same conditions as before. A plot of surface resistance versus implantation fluence is shown in Figure 5 for poly(styrene-acrylonitrile), and followed a similar dependence as the argon-implanted samples. Further test samples were implanted at one fluence only, 1×10^{17} ions/cm². Average film resistances for all of the implanted samples are shown in Table 2.

Due to the dissimilarity of the implanted polymers and metal electrodes, contact resistance was a potential problem.

Contact resistance was measured using the three-electrode test structure shown in Figure 6.⁶ In this method, the voltage drop across the contact in question was measured using a high-impedance voltmeter (a Keithley model 614). The contact resistance was equal to this voltage drop divided by the current. The contact resistances for several samples are shown in Table 3. Contact resistance to aluminum was very high, and in some cases increased on prolonged heating by a factor of three. Gold made a much better contact to the polymer and the contact didn't erode over time. The current-voltage plot of the boron-doped poly(styrene-acrylonitrile) was linear using gold electrodes.

Measurements of resistance versus temperature were conducted over two ranges, 50K to 300K and 298K to 373K. The results for PAN for the low-temperature range are shown in Figure 7. Over this wide temperature range, the temperature dependence was as follows:

$$\rho(T) = A \exp (B/T^{*0.5}),$$

where ρ is the resistivity and A and B are constants. The above temperature dependence implies a one-dimensional hopping mechanism for conduction, and has been observed in other ion-implanted polymers.^{7,8}

The conductivity was measured as a function of frequency in the frequency range from 10 hz to 20khz, shown in Figure 8. The frequency response was fit to a line obtained from the hopping model of conductivity in amorphous solids,⁸

$$\sigma(\omega) = \sigma_0 + A \omega^s,$$

where $\sigma(\omega)$ is the conductivity at a frequency ω . The data followed this behavior in a portion of the frequency range that was measured (50 hz to 1 khz), where s was a constant equal to 0.39.

An SEM photomicrograph of the boron-implanted polyacrylonitrile films revealed two distinct layers, one which was 0.26 micrometer thick and one which was 0.75 micrometer thick (Figure 9). The material was homogeneous on a one micron length scale. We interpreted the top layer to be the boron-implanted layer, which had a different morphology than the PAN layer due to interaction of the ions with the PAN. This interpretation was consistent with TRIM calculations, which predicted the mean range of the boron ions in PAN to be 0.225 micrometer.

The change of the resistance in a magnetic field is important for space applications. The resistance was found not to change appreciably in a magnetic field of 3 kilogauss,

which is an advantage of these materials over silicon diode temperature sensors.

Thermal and Ambient Stability of Boron-implanted Samples

Stability measurements were continued on boron-implanted poly(styrene-acrylonitrile) and NRL resins. Two quantities were considered in the stability measurements: the resistance change at 25°C and the change in the beta value (slope of $\ln R$ vs. $1/T$ plot). In general, the resistances and beta values were more stable after second and subsequent cycles.

Samples of boron-doped poly(styrene-acrylonitrile) and NRL resins were tested for stability to thermal cycling over the temperature range 25°C-100°C. The results are shown in Figure 10. After 48 cycles in air, the beta value remained within experimental error. The resistance values changed somewhat; the NRL resin had less change than the styrene-acrylonitrile polymer. Repeated cycling for another sample is shown in Figure 11.

Another test of thermal stability was conducted by heating the samples in air at successively higher temperatures for 15 minutes at each temperature, and measuring the resistance at the beginning and the end of each heating period. The results are plotted in Figures 12 and 13. The styrene-acrylonitrile samples showed a 4-8% increase in resistance (depending upon the temperature) after remaining at temperatures from 100-190°. After 195°, visible cracking occurred, accompanied by an increase in resistance. Implanted NRL resins had better thermal stability, exhibiting corresponding changes of from 0.4 to 3%.

Vacuum stability of the NRL resin was also better. Change in resistance after long-term vacuum heating at 120°C is shown in Figure 14. Films were heated in vacuum at 120° and removed at 5 and 30 hours for measurement. The beta values remained within experimental error, but the absolute resistance values increased on prolonged heating. The NRL resin had the smallest changes. Further work is required to determine whether this change continues, or whether it levels off. While this property is a disadvantage for high-temperature operation, it could be a convenient way of adjusting the film resistance to the desired values.

Long-term ambient stability was monitored for a sample of boron-implanted poly(styrene-acrylonitrile), implanted at 1×10^{17} ions/cm². The resistance of the film increased by 25% over a period of 140 days. The beta value of the film increased a total of 4% over that time period. Thus, while the resistance-temperature behavior was relatively stable

within the measurement accuracy, resistance increases occurred with time.

It should be noted that the sample kept for long-term stability had aluminum leads, which we now know degrade over time. Also, the above sample was stored in room air, in the presence of oxygen and moisture. Handling could have introduced sodium and other contaminants. In actual use the films would be covered with a passivation coating to prevent exposure to contaminants. There was not time during Phase I to isolate the factors which contributed to long-term resistance changes, as these changes appeared over a period of several months. Future work will target identification of stability in vacuum, as well as ambient stability of passivated samples and samples which have been annealed. Films which are approximately the thickness of the range of ions in the material may introduce better resistance uniformity and stability.

Pressure dependence of the resistance

To determine the effects of pressure on the resistance, a sample of implanted polymer on a glass slide with evaporated aluminum electrodes was placed in a chamber and pressurized with helium to a pressure of 29 psia. The resistance decreased with applied pressure as shown in Figure 15.

Resistance to Moisture and Solvents

Slides coated with boron-implanted NRL resin, poly(styrene-acrylonitrile), and polyacrylonitrile were suspended over boiling water. The resistance at 25° was measured before and after moisture exposure. The results are shown in Table 4. The NRL resin showed the smallest change. Finally, all three samples were immersed in the boiling water for two minutes. The PAN sample was cracked after the boiling water exposure, but the other two samples appeared unchanged except that there was adhesion loss between the electrodes and sample and sample and substrate. Even with cracking and adhesion loss, resistance changes were only about 2%.

The ion-implanted samples were extremely solvent resistant. Slides of all three polymers were dipped in N,N-dimethylformamide, then acetone. Dimethylformamide, in particular, is a strong organic solvent for the unimplanted polymers. The films were then dried in air. Resistance changes were within experimental error (0.5-0.6%).

Hall effect measurements

Because of the high impedance of the film, the method of Hall effect measurement shown in Figure 16a is susceptible to errors. If the sample leads are not directly opposite each other, a voltage drop will be measured due to misalignment. Figure 16b shows a simplified diagram of a sample geometry which corrects for these errors. When the magnetic field is turned off, the variable resistor shown in Figure 16b is tuned so that the voltage drop V_a is equal to zero. When the field is turned on, the measured voltage drop records the Hall voltage, which for a p-type sample is equal to:

$$V_a = I_x B_z / qtp,$$

where I_x = current
 B_z = magnetic flux density
 t = thickness
 q = electronic charge
 p = hole density.

Samples for the Hall effect measurements were prepared by the following technique. PAN was spin-coated from NMP/cyclohexanone solution, then baked on a hotplate to remove solvent. Shipley AZ1470J positive photoresist was spun on top of the polyacrylonitrile. The photoresist was exposed on a contact printer, using a mask of the geometry shown in Figure 16b. The exposed photoresist was removed with MF312 photoresist developer. The pattern was then transferred to the polyacrylonitrile layer by etching in an oxygen plasma barrel etcher. The photoresist was removed by rinsing in acetone. The thickness of the resulting polyacrylonitrile film was 3500 Angstroms. The films were implanted with boron ions (1×10^{17} ions/cm²) and the appropriate contacts were evaporated.

Hall effect measurements were difficult because of the high impedance of the sample. The results indicated n-type conductivity and a charge carrier density $> 7 \times 10^{16}$ cm⁻³. The large number of charge carriers implied a mobility-limited conductivity.

Control circuit for temperature measurement

Measuring the high resistances of the ion-implanted films requires a high impedance ohmmeter, which can be quite expensive. For practical, commercial applications, an inexpensive control circuit is required. Such a control circuit has been built as shown in Figure 17. In this circuit, 15 volts is placed across the sample in series with a 1 kilohm resistor. The current in the circuit is determined by the sample resistance (provided it is much larger than 1000 ohms); the voltage drop across the 1000 ohm

resistor is thus proportional to the resistance of the sample. The voltage is amplified by inexpensive, off-the-shelf components, and the output voltage (in the range of 10 volts) can be read by an inexpensive meter. In the unit which was built, all of the components except the power supply and the sample in Figure 17 were contained in a box which could be shielded from electrical interference, and the output was very stable.

IV. Discussion

The temperature dependence of the conductivity in ion implanted polymers has been attributed to a quasi one-dimensional hopping model of the conductivity. The model of conduction is as follows. Incoming ions create local damage in the film, stripping hydrogen off the polymer and creating dangling carbon bonds. In recombination, radical charge carriers are created. The film thus consists of regions of higher conductivity embedded in an insulating matrix, and the conductivity is dependent upon the hopping of the charge carriers from one conductive region to the other.

Wasserman et al. have determined from Hall effect measurements that polyacrylonitrile implanted with bromine ions has n-type conductivity.⁷ The results reported here are in agreement with Wasserman's, in that in both cases, the conductivity arises from a large number of charge carriers having a low mobility.

The pressure dependence which was measured is also in agreement with the hopping mechanism of conduction and a mobility-limited conduction mechanism. If the conductivity is limited by the ability of charge carriers to move from one conductive region to another across a nonconducting gap, then the effects of pressure are to decrease the distance between the conducting regions and to increase the conductivity. This behavior is the opposite of that of many crystalline semiconductors (such as germanium), in which the effect of decreasing the atomic distance is to increase the energy gap and increase the resistance.⁹

The final resistance and resistance-temperature characteristics were relatively independent of the percentage of acrylonitrile in the polymer. This result suggests that ion implantation at low energies results in a film structure which is quite different from the structure formed through low temperature pyrolysis. It is known that ion implantation creates graphite, whereas PAN which has been thermally pyrolyzed to an intermediate resistivity consists of nitrogen-containing conjugated rings.¹⁰

It is interesting that both poly(styrene-acrylonitrile) and PAN had relatively low glass transition temperatures (46°

and 85°C, respectively), and yet the implanted polymer had good stability to recycling at temperatures above the Tg. The NRL resin was somewhat more stable, possibly due to a higher melting temperature. It is likely that samples which have a thickness equal to the mean range of ions in the material will have better thermal stability, because hardening of the film by the ions would result in a uniform composition which does not rest on a softer, unimplanted polymer base.

V. Summary

We have demonstrated temperature sensors formed from several nitrile-containing polymers which can be applied from solution onto a substrate, then subsequently ion implanted to have conductivity in the kilohm to megaohm/square range. If desired, the films can be patterned before implantation to small geometries by lithographic procedures.

The resulting films have a large, negative temperature coefficient of resistance. The resistance-temperature response of some samples is reproducible and retraceable within experimental error over multiple cycles. Limited aging experiments that were conducted during Phase I show some shifts in absolute resistance values (rather than R/T slopes) over a period of several months, and suggestions have been made as to means of improving the stability.

The film-type temperature sensors demonstrated during Phase I have a number of advantageous properties. First of all, they have high resistance, which means that lead resistance is negligible. A second advantage is that the films are radiation-hard, having already been exposed to radiation during the fabrication process. Finally, the coatings are extremely durable and solvent resistant, and exhibit no change of resistance in a magnetic field.

In conclusion, we demonstrated a new type of temperature sensors which have advantages over temperature sensors which are currently available. The devices demonstrated during Phase I could be deposited onto expensive electrical components such as high power transistors as a protective measure against overheating. Other potential applications include the monitoring of processing during the manufacture of microelectronics circuits, and the mapping of thermal gradients across a surface.

References

1. M. S. Dresselhaus, B. Wasserman, and G. E. Wnek, "Ion Implantation of Polymers," Mat. Res. Soc. Symp. Proc. 27, p. 413 (1984).
2. R. E. Giedd, J. Shipman, and M. Murphy, "Electronic Properties of Ion Implanted Polymer Films," Mat. Res. Soc. Symp. Proc. Vol. 147 (1989).
3. R. E. Giedd, M. G. Moss, and M. Craig, "Temperature Sensitive Ion-Implanted Films," presented at IBBM conf. in Knoxville, TN, September 1990, to be published in Nucl. Instr. and Methods.
4. J. F. Ziegler, J. P. Biersack and U. Littmark, "The Stopping and Range of Ions in Solids," Pergamon Press, Oxford (1985).
5. S. P. Herish, S. Brock, and P. L. Grady, "Conducting Polymers by Ion Implantation," J. Polym. Phys. Ed. 22, p. 1349 (1984).
6. T. J. Faith, R. S. Irven, S. K. Plante, and J. J. O'Neill, Jr., J. Vac. Sci. Technol. A1 (2), p. 443 (1983).
7. B. Wasserman, G. Braunstein, M. S. Dresselhaus, and G. E. Wnek, "Implantation-Induced Conductivity of Polymers," Mat. Res. Soc. Symp. Proc. 27, p. 423 (1984).
8. D. Redfield, Phys. Rev. B30 (26), p. 1319 (1973).
9. J. I. Pankove, Optical Processes in Semiconductors, Dover Publications, New York (1971).
10. H. Teoh, P. D. Metz, and W. G. Wilhelm, "Electrical Conductivity of Pyrolyzed Polyacrylonitrile," Mol. Cryst. Liq. Cryst., 83, p. 297 (1982).

Table 1
POLYMERS TESTED DURING PHASE I

<u>Polymer</u>	<u>Abbreviation</u>
Poly(acrylonitrile-methyl methacrylate) (94/6)	PAN
Poly(styrene-co-acrylonitrile) (80/20)	SA
Thermally crosslinkable resin	NRL
Polysulfone	PS
Polyazomethine	PAM

Table 2
RESISTANCE AND β VALUES
FOR IMPLANTED POLYMER FILMS

<u>Polymer</u>	<u>Ion</u>	<u>$R_s(298\text{ K})^*$</u> M Ω /square	<u>ρ</u> ohm cm	<u>β</u>
Polyacrylonitrile	Ar ⁺	79.	530.	2000
"	B ⁺	1.0	23.	1112
Polystyrene-acrylonitrile	Ar ⁺	51.	340	1723
"	B ⁺	2.3	51	1645
Phthalonitrile-term. resin	B ⁺	1.8	41	1501
"	As ⁺	0.46	3.4	980
Polysulfone	Ar ⁺	56	370	1738
Polyazomethine	Ar ⁺	1000	6700	-

* $R_s = (R/d \text{ in ohm/mm}) \times 25.4$, averages of all samples at a single fluence.

Table 3
CONTACT RESISTANCE OF BORON-DOPED POLYMERS

Polymer	electrode	R_c
Styrene-acrylonitrile	Al	12 k Ω
" after extended heating	"	190 k Ω
"	Au	160 Ω
Phthalonitrile resin	Al	7 k Ω
" after extended heating	"	100 k Ω
"	Au	<30 Ω

Table 4
RESISTANCE CHANGES DUE TO MOISTURE EXPOSURE

Polymer	%Change*	Appearance**
SA, B+	-7.4%	unchanged
NRL, B+	-0.9%	unchanged
PAN, B+	+4.1%	cracked

*% change in resistance after 15 minutes exposure to steam

** appearance of film after boiling in water for 2 minutes

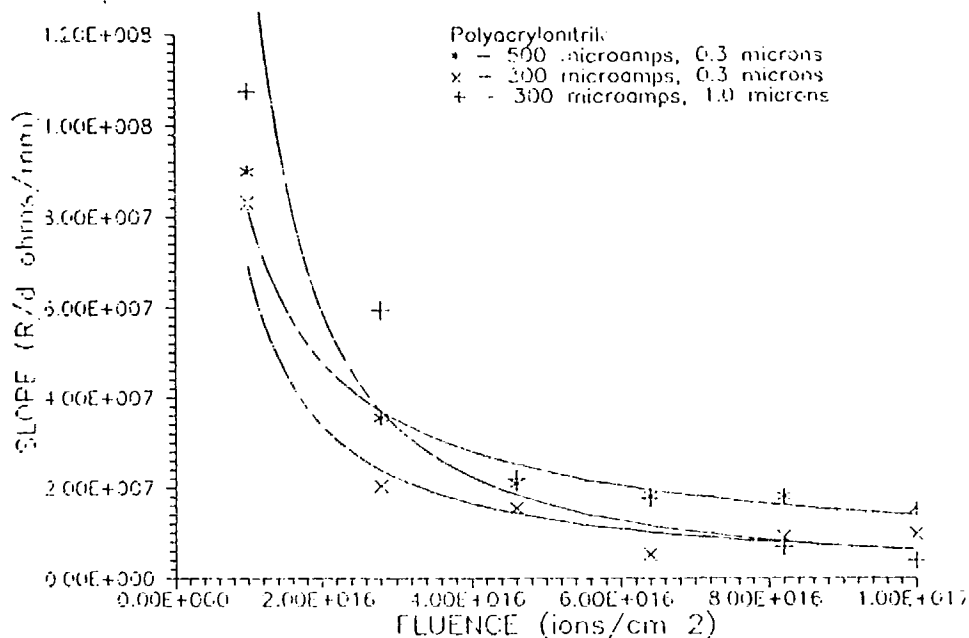


FIGURE 1: Resistance as a function of argon ion fluence for polyacrylonitrile films. *, 0.3 micron film, 500 microamps beam current; x, 0.3 micron film, 300 microamps beam current; +, 1.0 micron film, 300 microamps beam current.

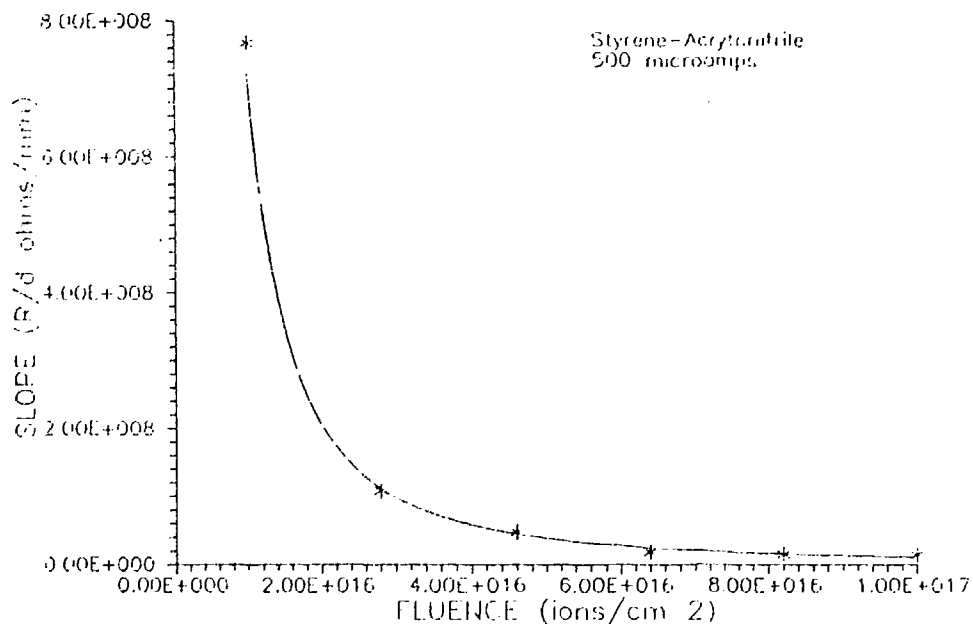


FIGURE 2: Resistance as a function of argon ion fluence for ion implanted films of polystyrene-acrylonitrile, 1 micron film, 500 microamps beam current.

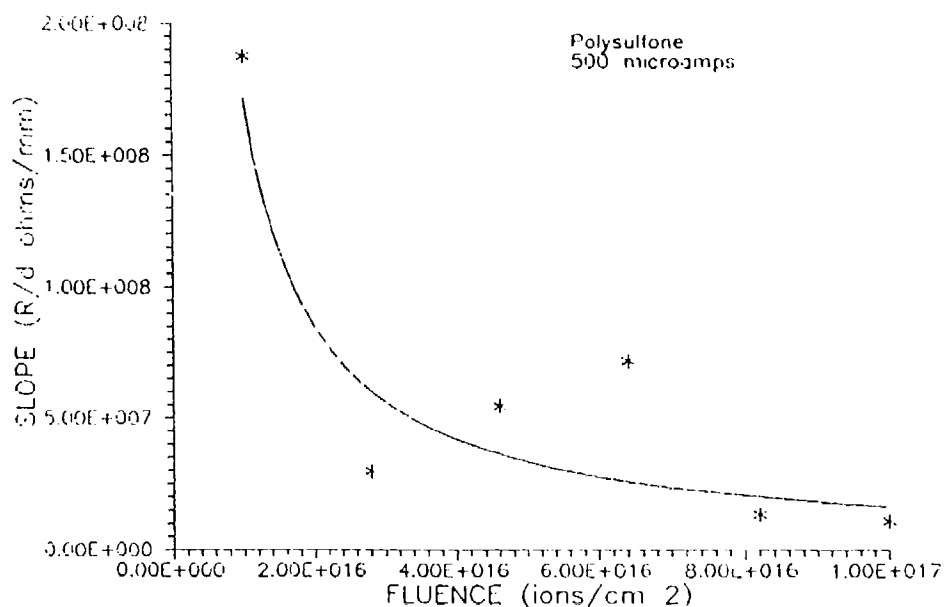


FIGURE 3: Resistance as a function of argon ion fluence for ion implanted films of polysulfone, 1 micron film, 500 microamps beam current.

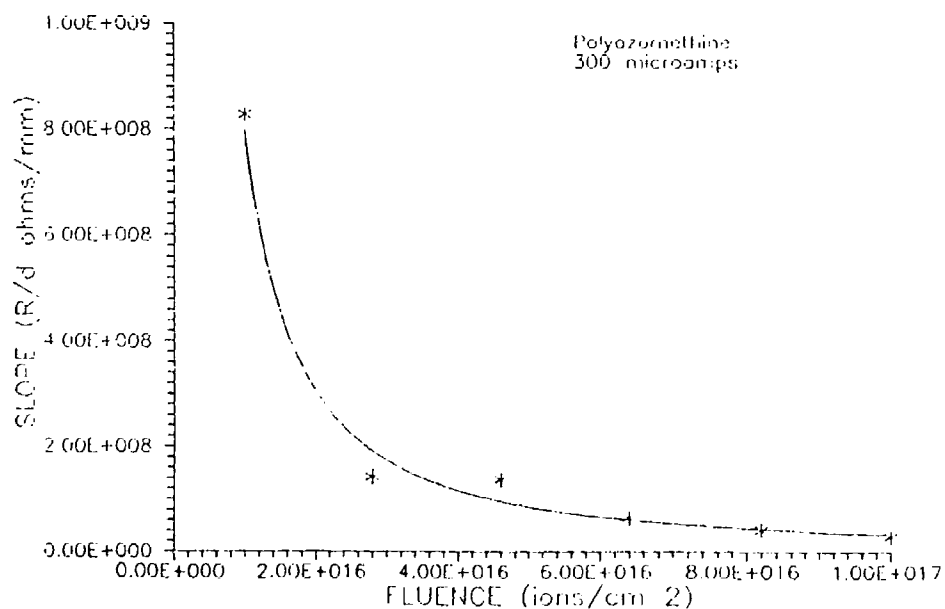


FIGURE 4: Resistance as a function of argon ion fluence for ion implanted films of a block polymer containing azomethine segments, 1 micron film, 300 microamps beam current.

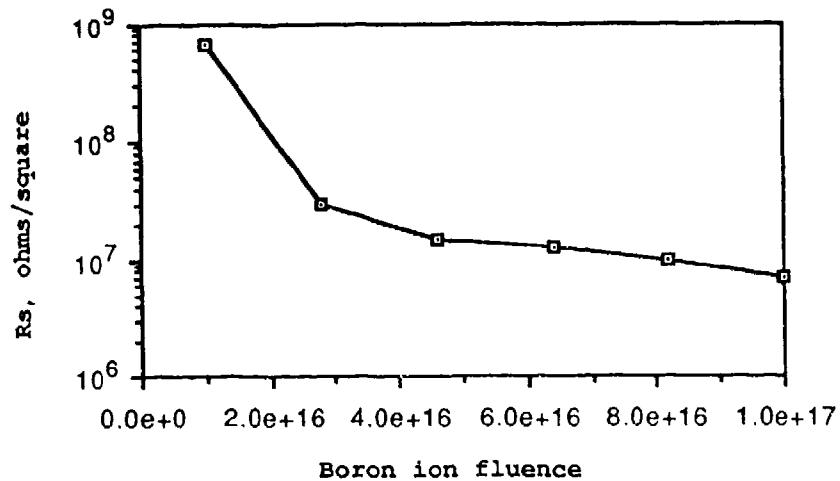


Figure 5: Resistance as a function of fluence for boron implanted poly(styrene-acrylonitrile) (50 KeV ions).

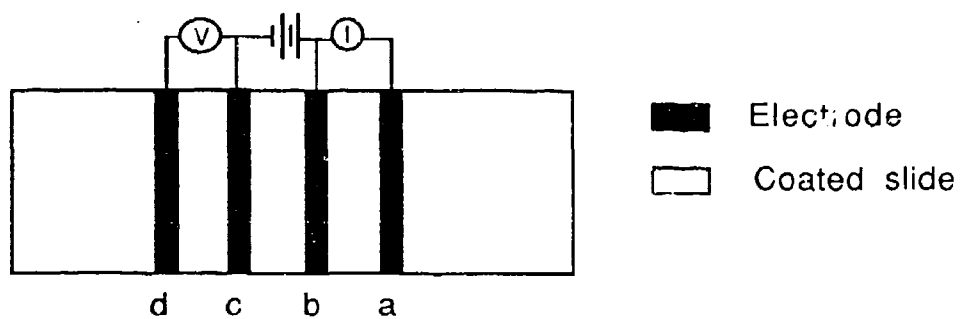


Figure 6: Kelvin test structure to measure contact resistance.

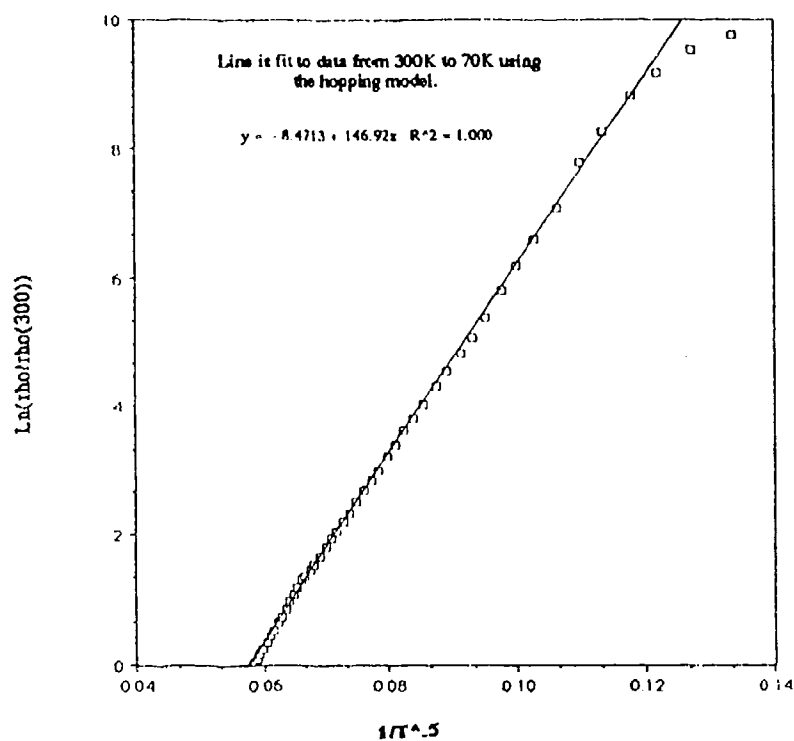


Figure 7: Temperature dependence of resistance at cryogenic temperatures for polyacrylonitrile films implanted with boron with a fluence of 1×10^{17} ions/cm².

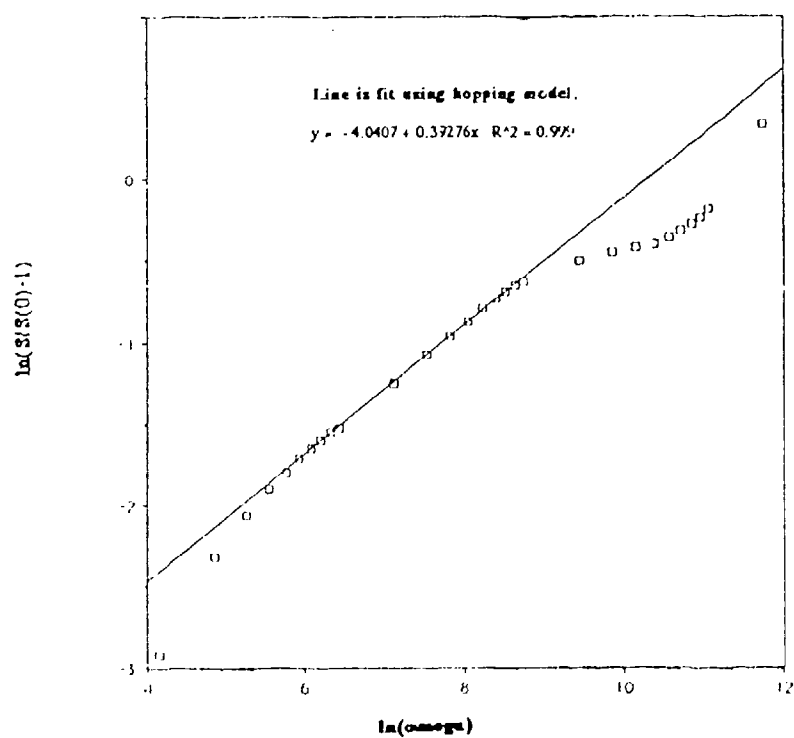


Figure 8: Frequency dependence of the conductivity of boron implanted polyacrylonitrile.



Figure 9: SEM of the physical morphology on the 1 μm length scale of boron-implanted PAN. Specimen is dry-fractured and viewed on edge. This sample was irradiated to a fluence of 1.2×10^{17} ions/cm² at a beam energy of 50 keV and a beam current of 300 μA . a and b, upper stratum of boron implanted PAN; c, lower stratum of native PAN; d, SiO₂ substrate. Bar, 1 μm .

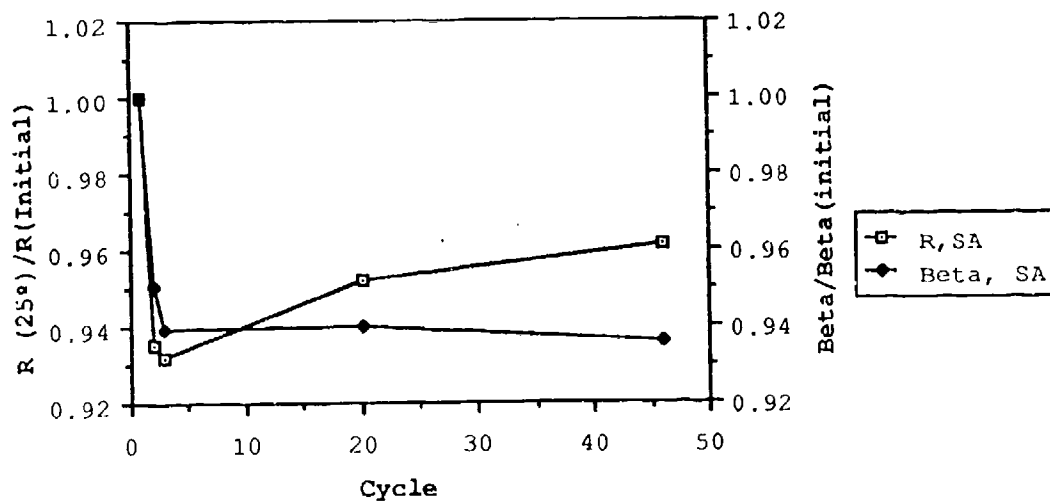
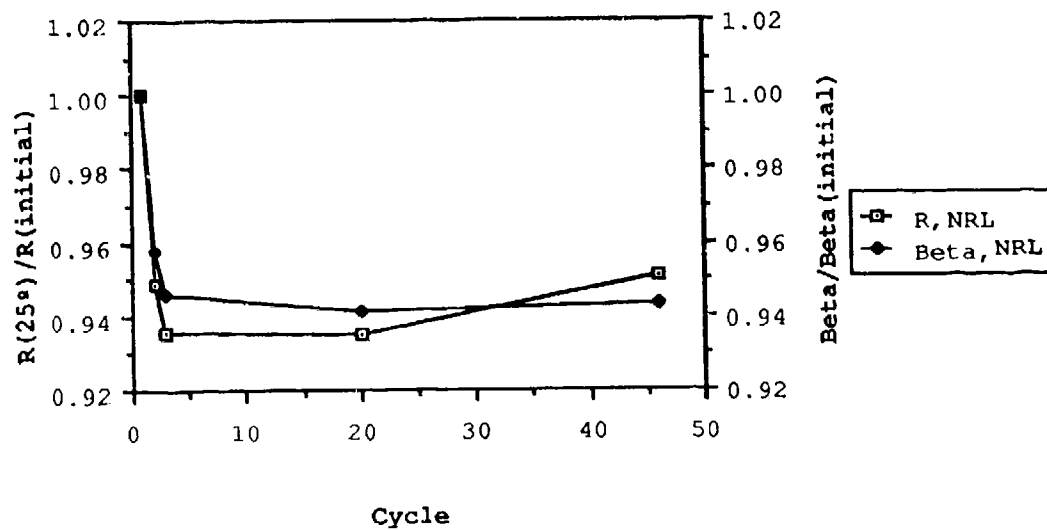


Figure 10: Changes in 25° resistance and beta values after repeated thermal cycling from 25°C to 100°C of boron-implanted NRL resin (top) and poly(styrene-acrylonitrile) (bottom).

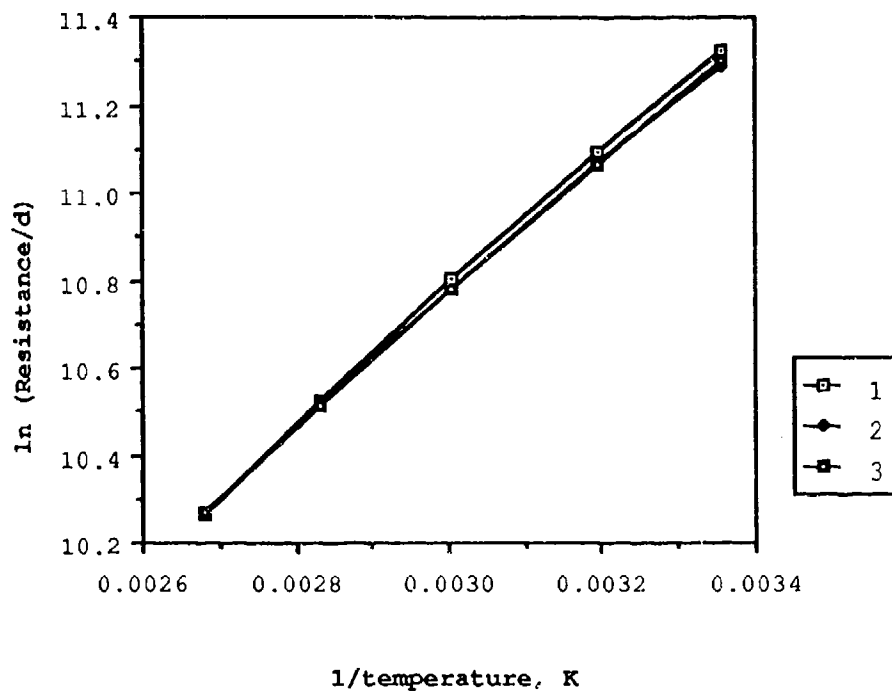


Figure 11: Measurement of resistance versus temperature for NRL resin, showing typical stabilization for second and third measurement.

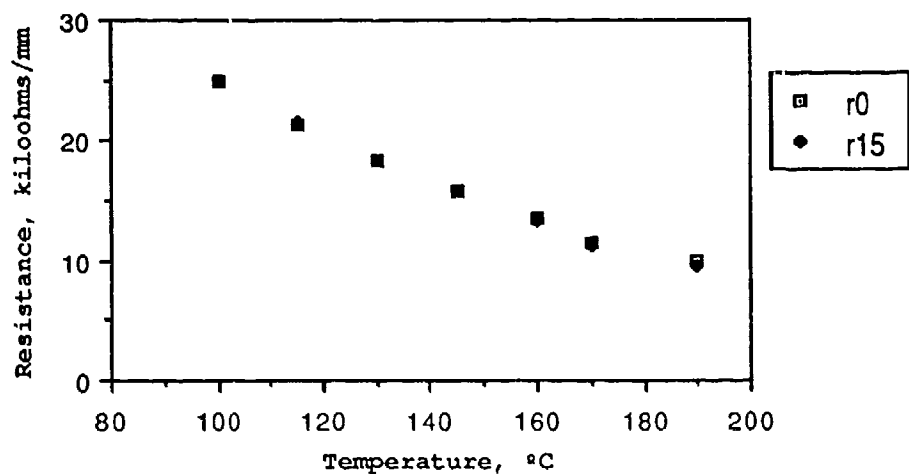


Figure 12: Resistance as a function of temperature for a boron-implanted NRL resin sample which has been heated for 15 minutes at each temperature. \square , resistance measured at the beginning of the heating period; \bullet , resistance measured at the end of the period.

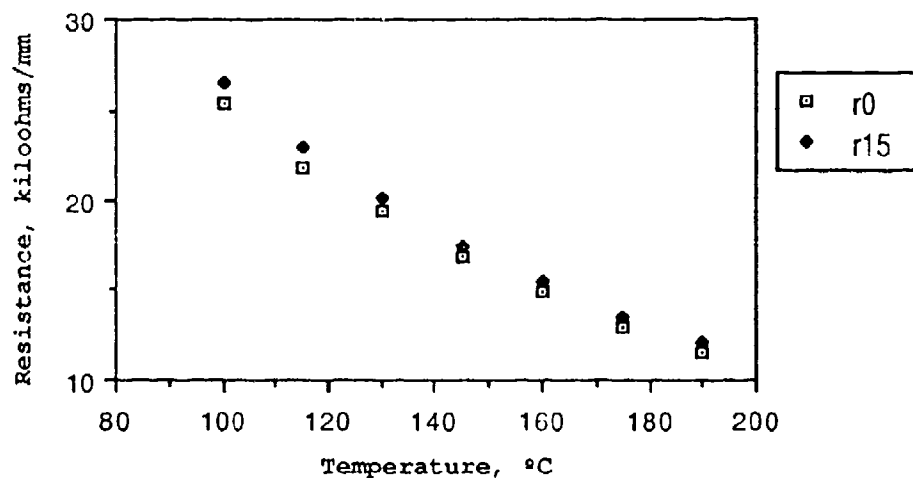


Figure 13: Resistance as a function of temperature for a boron-implanted SA resin sample which has been heated for 15 minutes at each temperature. \square , resistance measured at the beginning of the heating period; \bullet , resistance measured at the end of the period.

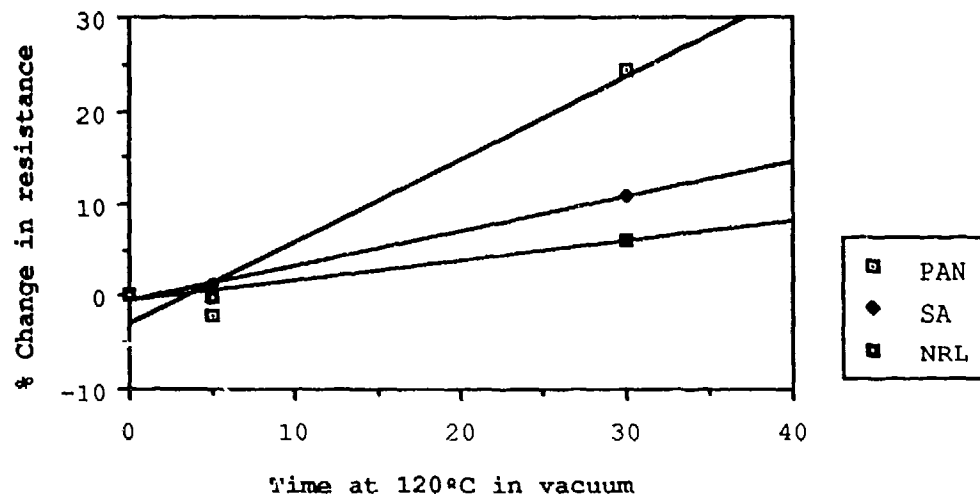


Figure 14: Percentage change in 25°C resistance after heating at 120° in vacuum.

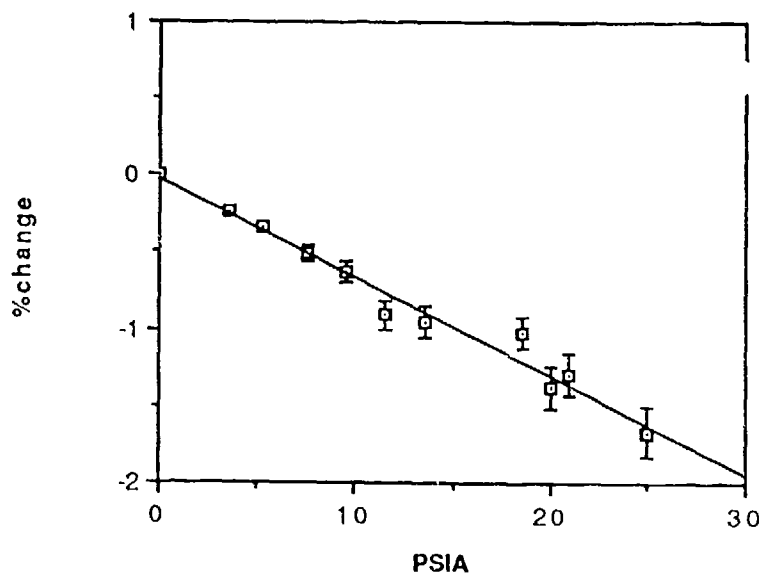


Figure 15: Changes of resistivity of boron implanted polyacrylonitrile due to applied helium pressure.

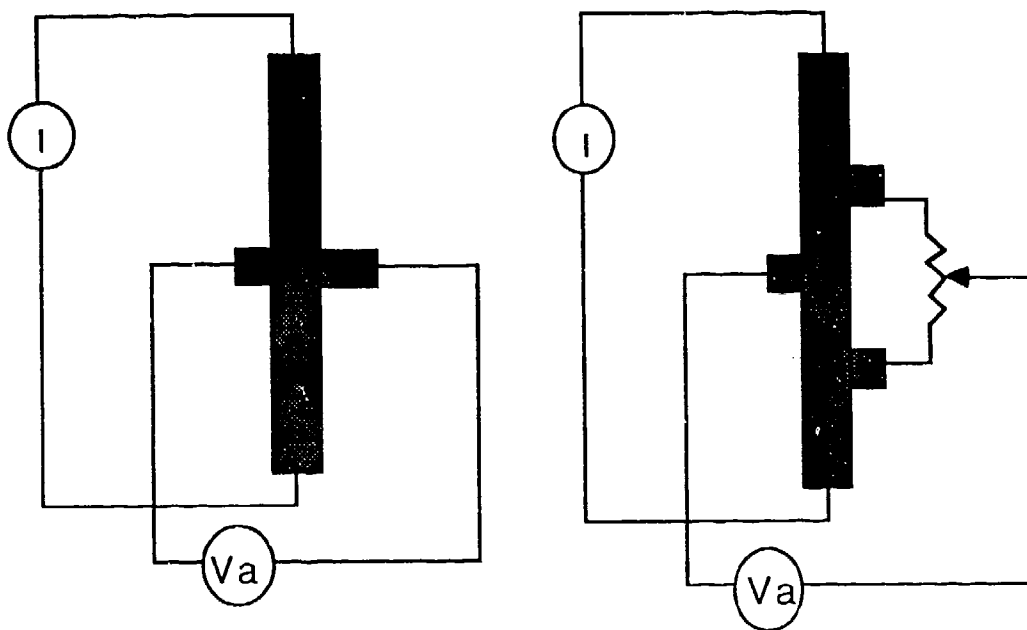


Figure 16: Left, Hall effect configuration. Right, Configuration which compensates for misalignment of electrodes.

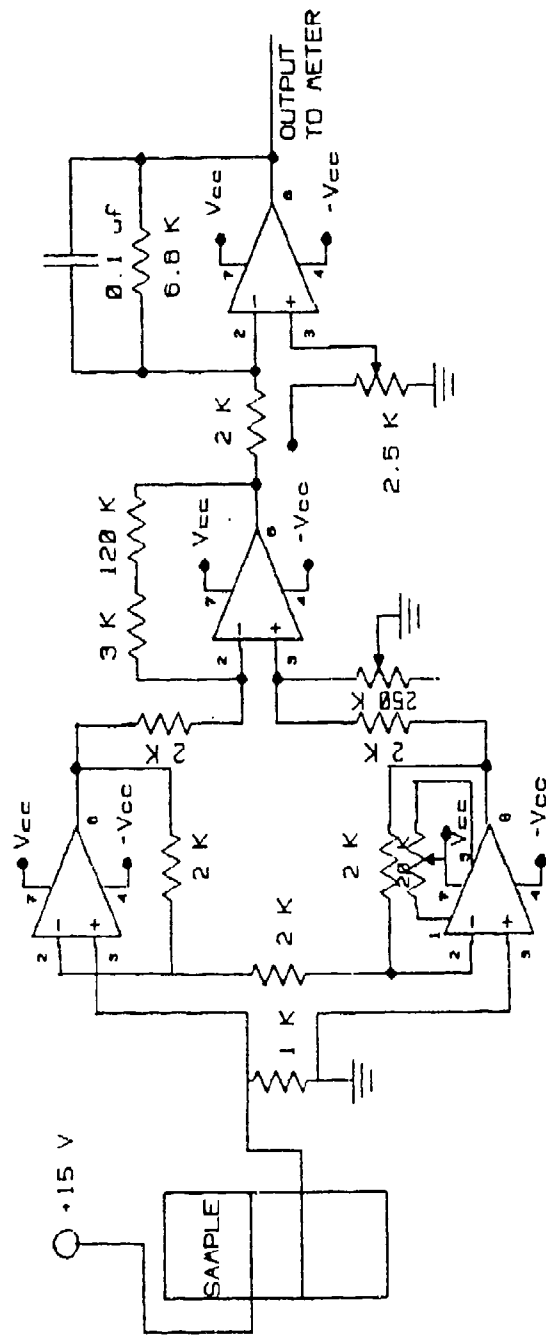


Figure 17: Control circuit for temperature measurement.